Chemical Science



EDGE ARTICLE

View Article Online
View Journal | View Issue



Cite this: *Chem. Sci.*, 2015, **6**, 6496

# Catalytic two-electron reduction of dioxygen catalysed by metal-free [14]triphyrin(2.1.1)†

Kentaro Mase,[a] Kei Ohkubo,[ab] Zhaoli Xue,[c] Hiroko Yamada*[c] and Shunichi Fukuzumi*[abd]

Received 8th July 2015
Accepted 2nd August 2015

DOI: 10.1039/c5sc02465j

www.rsc.org/chemicalscience

The catalytic two-electron reduction of dioxygen ($O_2$) by octamethylferrocene ($Me_8Fc$) occurs with a metal-free triphyrin (HTrip) in the presence of perchloric acid ($HClO_4$) in benzonitrile (PhCN) at 298 K to yield $Me_8Fc^+$ and $H_2O_2$. Detailed kinetic analysis has revealed that the catalytic two-electron reduction of $O_2$ by $Me_8Fc$ with HTrip proceeds *via* proton-coupled electron transfer from $Me_8Fc$ to HTrip to produce $H_3Trip^{\bullet+}$, followed by a second electron transfer from $Me_8Fc$ to $H_3Trip^{\bullet+}$ to produce $H_3Trip$, which is oxidized by $O_2$ *via* formation of the $H_3Trip/O_2$ complex to yield $H_2O_2$. The rate-determining step in the catalytic cycle is hydrogen atom transfer from $H_3Trip$ to $O_2$ in the $H_3Trip/O_2$ complex to produce the radical pair ($H_3Trip^{\bullet+}$ $HO_2^{\bullet}$) as an intermediate, which was detected as a triplet EPR signal with fine-structure by the EPR measurements at low temperature. The distance between the two unpaired electrons in the radical pair was determined to be 4.9 Å from the zero-field splitting constant (*D*).

## Introduction

Utilization of natural energy to produce chemical energy consisting of earth-abundant elements is an essential technology for building a society based on the sustainable use of materials. Hydrogen peroxide ($H_2O_2$) produced by two-electron reduction of $O_2$ is a versatile and environmentally benign oxidant, which is widely used on a large industrial scale.[1,2] Furthermore, $H_2O_2$ has been proposed as a sustainable energy carrier that can be used in fuel cells, where direct and efficient conversion of chemical to electrical energy is required.[3–5] However, the anthraquinone process, currently used to produce $H_2O_2$ in industry, requires potentially explosive hydrogen and a noble metal catalyst.[6] Extensive efforts have so far been devoted to provide an alternative way to produce $H_2O_2$ photochemically or thermally without the use of noble metal catalysts.[7–13] In many cases, redox-active transition metal-based complexes such as cobalt,[14–23] iron,[24–27] and copper complexes,[28–31] have been employed as $O_2$ reduction catalysts, because triplet $O_2$ is inactive towards organic compounds due to spin restriction in the absence of an appropriate catalyst.[32]

Recently, nitrogen-doped carbon materials have attracted increasing attention as an efficient metal-free catalyst for the catalytic reduction of $O_2$.[33–35] However, the catalytic mechanism has yet to be well understood, because few spectroscopic studies to detect reaction intermediates in a catalytic cycle have been performed on heterogeneous systems. In homogeneous systems, reduced flavin analogues involved in flavoenzymes have so far been known to play a pivotal role in the catalytic reduction of $O_2$, which is a key step of biological oxidation.[36,37] In particular, the deprotonated states of reduced flavin analogues, which are thermodynamically more able to reduce $O_2$ *via* an electron-transfer process, are considered to be a reactive intermediate in the reduction of $O_2$.[38]

On the other hand, Girault and coworkers recently reported that the free base porphyrin has the ability to catalyse the two-electron reduction of $O_2$ using one-electron reductants such as ferrocene at liquid–liquid interfaces.[39] In such systems, although the catalytic mechanism of metal-free organocatalysts has yet to be clarified, the oxidation state of the organocatalyst is thought to remain the same during the catalytic reduction of $O_2$. Thus, no electron-transfer reduction of organic catalysts has been reported in relation to the catalytic reduction of $O_2$.

In this context, Nocera and coworkers recently reported the stabilization of the peroxide dianion within the cavity of a hexacarboxamide cryptand,[40] where strong hydrogen bond donors are arranged to completely surround the peroxide dianion with a partial positive charge. This result provides support for the proposal that metal-free organocatalysts, which have multiple hydrogen bonding moieties, can efficiently catalyse $O_2$ reduction.

[a]Department of Material and Life Science, Graduate School of Engineering, ALCA and SENTAN, Japan Science and Technology Agency (JST), Osaka University, Suita, Osaka 565-0871, Japan. E-mail: fukuzumi@chem.eng.osaka-u.ac.jp

[b]Department of Chemistry and Nano Science, Ewha Womans University, Seoul 120-750, Korea

[c]Graduate School of Materials Science, Nara Institute of Science and Technology, CREST, Japan Science and Technology Agency (JST), Ikoma, Nara 630-0192, Japan. E-mail: hyamada@ms.naist.jp

[d]Faculty of Science and Engineering, ALCA, SENTAN, Japan Science and Technology Agency (JST), Meijo University, Nagoya, Aichi 468-0073, Japan

† Electronic supplementary information (ESI) available: Spectroscopic, kinetic and DFT data. See DOI: 10.1039/c5sc02465j

 

We report herein the catalytic two-electron reduction of $O_2$ by an one-electron reductant, octamethylferrocene ($Me_8Fc$), with metal-free [14]triphyrin(2.1.1) (denoted as HTrip in Chart 1)[41] in the presence of $HClO_4$ in benzonitrile (PhCN) at 298 K. The catalytic mechanism for the $O_2$ reduction by $Me_8Fc$ is clarified on the basis of a detailed kinetic study. Proton-coupled electron-transfer reduction of HTrip by $Me_8Fc$ results in the formation of the reduced state of HTrip, and this resulting reduced HTrip is oxidized by $O_2$ to reproduce HTrip, indicating that HTrip acts as a metal-free catalyst for the reduction of $O_2$ by $Me_8Fc$ in the presence of $HClO_4$ in PhCN. This discovery of a reactive intermediate in the catalytic $O_2$ reduction with a molecular organic catalyst provides valuable insight into the development of an efficient metal-free catalyst for the reduction of $O_2$.

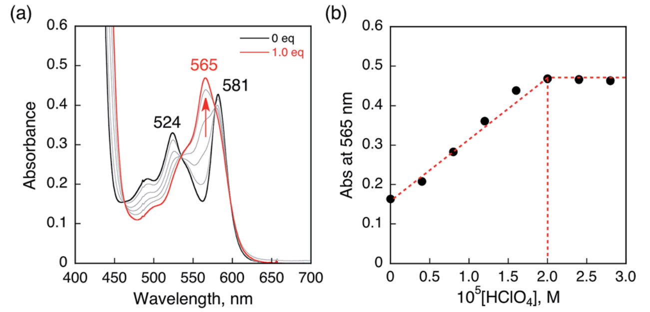


Fig. 1 (a) Absorption spectral changes of HTrip ($2.0 \times 10^{-5}$ M) upon the addition of $HClO_4$ in air-saturated PhCN at 298 K. (b) Absorbance change profile at 565 nm.

## Results and discussion

### Protonation of HTrip with $HClO_4$

HTrip was protonated by addition of perchloric acid ($HClO_4$) to an air-saturated benzonitrile (PhCN) solution of HTrip. The characteristic absorption bands for HTrip at 524 and 581 nm decreased in intensity, with an increase in the absorption band at 565 nm, exhibiting clean isosbestic points, as shown in Fig. 1a. As can be seen in Fig. 1b, the absorbance change at 565 nm is saturated in the presence of 1 equiv. of $HClO_4$. Thus, HTrip is protonated to afford $H_2Trip^+$, as given by eqn (1).

$$\mathrm{HTrip} + \mathrm{H}^+ \rightarrow \mathrm{H_2Trip}^+ \quad (1)$$

The p$K_a$ value of $H_2Trip^+$ in PhCN was estimated to be 15.6 from the titration of HTrip with trifluoroacetic acid (TFA), as shown in Fig. S1 in the ESI.† The p$K_a$ value of $H_2Trip^+$ is slightly larger than that of free base porphyrin analogues.[42] There is no further protonation due to strong repulsion between NH protons in the small macrocyclic ligand, as reported previously.[41]

### Electrochemical measurements of HTrip in the presence of $HClO_4$

Electrochemical measurements of HTrip were performed in deaerated PhCN containing 0.10 M $TBAPF_6$, as shown in Fig. 2. A cyclic voltammogram of HTrip exhibits reversible reduction waves at $E_{1/2} = -1.13$ and $-1.37$ V (*vs.* SCE), which correspond to the first and second one-electron reduction of HTrip. The first one-electron oxidation occurs at $E_{1/2} = 1.04$ V, which is followed by an irreversible oxidation (Fig. 2a). The formation of $HTrip^{\bullet-}$ was detected by UV-vis absorption spectra in the electrochemical reduction of HTrip at a controlled potential of $-1.25$ V *vs.* SCE in the thin-layer cell, as shown in Fig. S2 in the ESI.† By addition of $HClO_4$, the first reduction potential of HTrip was positively shifted from $E_{1/2} = -1.13$ V to $-0.31$ V (*vs.* SCE) because of the protonation of HTrip, but the reduction became irreversible (Fig. 2b). In such a case, proton-coupled electron transfer from an electron donor with the one-electron oxidation potential, which is less negative than $-0.31$ V, to HTrip may be thermodynamically feasible (*vide infra*).

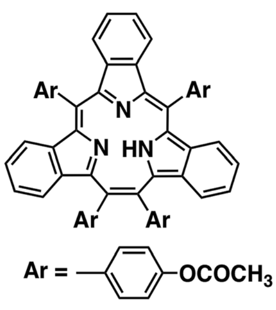


Chart 1 Structure of HTrip.

### Electron-transfer reduction of HTrip in the presence of $HClO_4$

No electron transfer from $Me_8Fc$ to HTrip occurred in the absence of $HClO_4$ in PhCN at 298 K, as indicated by the more negative $E_{1/2}$ value of HTrip ($-1.13$ V *vs.* SCE) as compared with that of $Me_8Fc$ ($-0.04$ V *vs.* SCE).[8] However, the addition of more than two equiv. of $HClO_4$ to a deaerated PhCN solution of $Me_8Fc$ and HTrip resulted in the appearance of an absorption band at 738 nm due to $H_3Trip$ with clean isosbestic points, as shown in Fig. 3. It should be noted that no electron transfer from $Me_8Fc$ to $H_2Trip^+$ occurred in the presence of one equiv. of $HClO_4$, as shown in Fig. 3b. These results indicate that uphill electron transfer from $Me_8Fc$ to $H_2Trip^+$ is coupled with protonation of $H_2Trip^\bullet$ to produce $H_3Trip^{\bullet+}$, followed by fast electron transfer from $Me_8Fc$ to $H_3Trip^{\bullet+}$ to yield $H_3Trip$. Thus, the second protonation in fact occurs by coupling with reduction of $H_2Trip^+$ (*i.e.* $H_3Trip^{\bullet+}$ is accessible but not $H_3Trip^{2+}$). The stoichiometry of the overall reaction is given in Scheme 1.

The rate of proton-coupled electron-transfer reduction of $H_2Trip^+$ ($k_{et}$) to form $H_3Trip^{\bullet+}$ was determined from the dependence of the observed rate constant ($k_{obs}$) on concentrations of $Me_8Fc$ and $HClO_4$, as shown in Fig. 4. The $k_{obs}$ value was determined from the increase in absorbance at 738 nm due to $H_3Trip$, which obeyed first-order kinetics (Fig. S3 in the ESI†). The $k_{obs}$ value increased linearly with increasing concentrations of $Me_8Fc$ and $HClO_4$, as shown in Fig. 5. Thus, the rate of formation of $H_3Trip$ is given by eqn (2).

$$\mathrm{d[H_3Trip]/d}t = k_{et}[\mathrm{H_2Trip^+}][\mathrm{HClO_4}][\mathrm{Me_8Fc}] \quad (2)$$

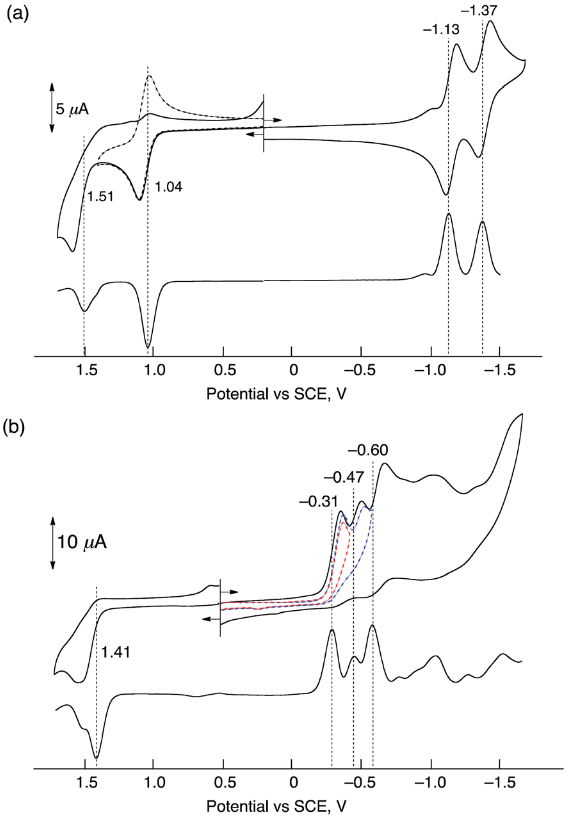


Fig. 2 Cyclic voltammograms (upper) and differential pulse voltammograms (lower) of deaerated PhCN solutions of HTrip ($1.0 \times 10^{-3}$ M) recorded in the presence of $TBAPF_6$ (0.10 M) (a) without $HClO_4$ and (b) with $HClO_4$ ($1.0 \times 10^{-2}$ M); sweep rate: 100 mV $s^{-1}$ for CV and 4 mV $s^{-1}$ for DPV.

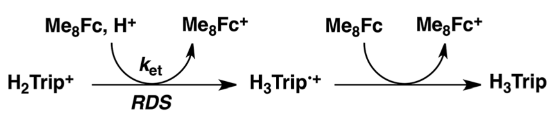


Scheme 1

The $k_{et}$ value is determined from the slope of the linear plot of $k_{obs}$ *vs.* [$Me_8Fc$] and [$HClO_4$] to be $(9.8 \pm 0.2) \times 10^4$ $M^{-2}$ $s^{-1}$. The $k_{et}$ value of the proton-coupled electron-transfer reduction of $H_2Trip^+$ by $Me_{10}Fc$ was also determined from the slope of the linear plot of $k_{obs}$ *vs.* [$Me_{10}Fc$] and [$HClO_4$] to be $(3.1 \pm 0.3) \times 10^5$ $M^{-2}$ $s^{-1}$ (Fig. S4–S6 in the ESI†). The $k_{et}$ value for $Me_{10}Fc$ is larger than that for $Me_8Fc$ because $Me_{10}Fc$ ($E_{ox} = -0.08$ V *vs.* SCE) is a stronger electron donor than $Me_8Fc$ (−0.04 V *vs.* SCE).[28]

The formation of $H_3Trip$ was also confirmed by the electrochemical reduction of $H_2Trip^+$ monitored by the UV-vis spectral change at an applied potential of −0.30 V *vs.* SCE in the thin-layer cell, as shown in Fig. S7 (in the ESI†). The product obtained after the electrochemical reduction of $H_2Trip^+$ at −0.30 V displayed the characteristic absorption band at 738 nm. The same absorption band was seen in the chemical reduction of $H_2Trip^+$ by $Me_8Fc$ in the presence of $HClO_4$ (Fig. 2).

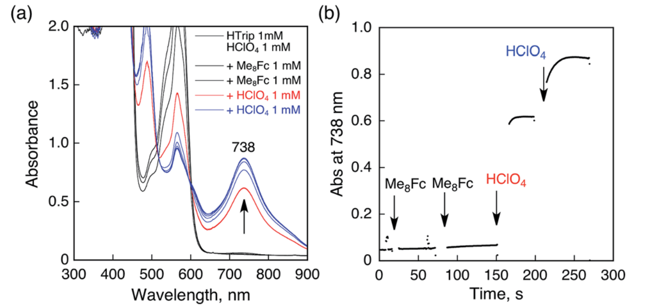


Fig. 3 (a) Absorption spectral changes upon addition of $Me_8Fc$ ($1.0 \times 10^{-3}$ and $2.0 \times 10^{-3}$ M) to a deaerated PhCN solution of $H_2Trip^+$ ($1.0 \times 10^{-3}$ M) in the presence of $HClO_4$ ($1.0 \times 10^{-3}$ M) at 298 K in a quartz cuvette (light path length = 1 mm) (black); absorption spectral change upon addition of $HClO_4$ ($1.0 \times 10^{-3}$ M) to the solution indicated by the black line (red); absorption spectral change upon addition of $HClO_4$ ($1.0 \times 10^{-3}$ M) to the solution indicated by the red line (blue). (b) Absorption change at 738 nm upon addition of various concentrations of $Me_8Fc$ and $HClO_4$.

When $O_2$ was introduced to a deaerated PhCN solution of $H_3Trip$ produced by the proton-coupled electron transfer from $Me_8Fc$ to HTrip in the presence of $HClO_4$, the absorption band at 738 nm due to $H_3Trip$ was immediately changed to a new absorption band at 720 nm, which can be attributed to the formation of the $O_2$ complex, as shown in Scheme 2 (*vide infra*). Subsequently, this spectrum decreased gradually, accompanied by the regeneration of HTrip as shown in Fig. 6. This indicates that $H_3Trip$ was readily oxidized by $O_2$ to produce HTrip and $H_2O_2$ (Scheme 2).

### Catalytic two-electron reduction of $O_2$ by $Me_8Fc$ with HTrip in the presence of $HClO_4$

The proton-coupled electron-transfer reduction of HTrip by $Me_8Fc$ (Scheme 1) and the oxidation of the resulting reduced HTrip ($H_3Trip$) by $O_2$ (Scheme 2) indicate that HTrip acts as a metal-free catalyst for the reduction of $O_2$ by $Me_8Fc$ in the presence of $HClO_4$ in PhCN. Indeed, the addition of $Me_8Fc$ to air-saturated PhCN at 298 K containing a catalytic amount of

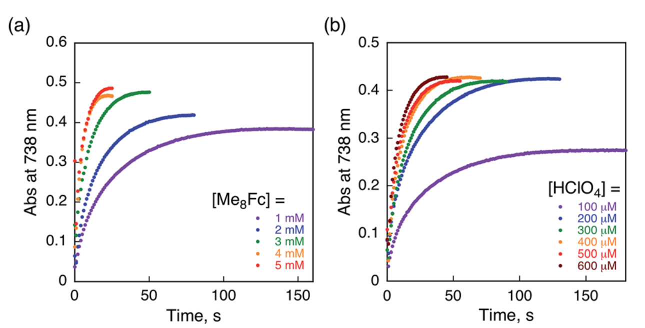


Fig. 4 Time profiles of absorbance at 738 nm due to $H_3Trip$ in the reduction of $H_2Trip^+$ ($2.5 \times 10^{-5}$ M) (a) by various concentrations of $Me_8Fc$ in the presence of $HClO_4$ ($3.0 \times 10^{-4}$ M) and (b) by $Me_8Fc$ ($2.0 \times 10^{-3}$ M) in the presence of various concentrations of $HClO_4$ in deaerated PhCN at 298 K.

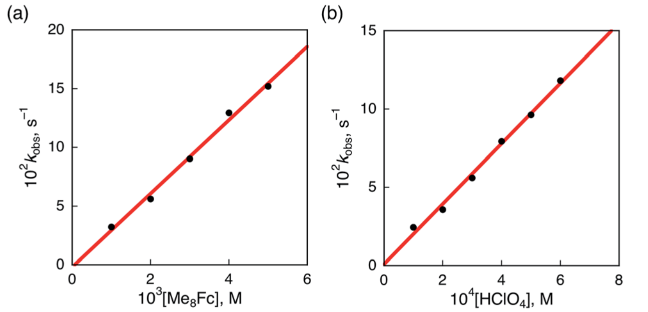


Fig. 5 (a) Plot of $k_{obs}$ *vs.* [$Me_8Fc$] for the reduction of $H_2Trip^+$ ($2.5 \times 10^{-5}$ M) by various concentrations of $Me_8Fc$ in the presence of $HClO_4$ ($3.0 \times 10^{-4}$ M) in PhCN at 298 K. (b) Plot of $k_{obs}$ *vs.* [$HClO_4$] for the reduction of $H_2Trip^+$ ($2.5 \times 10^{-5}$ M) by $Me_8Fc$ ($2.0 \times 10^{-3}$ M) in the presence of various concentrations of $HClO_4$ in deaerated PhCN at 298 K.

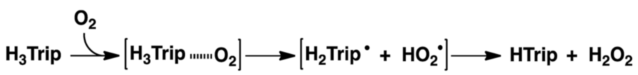


Scheme 2

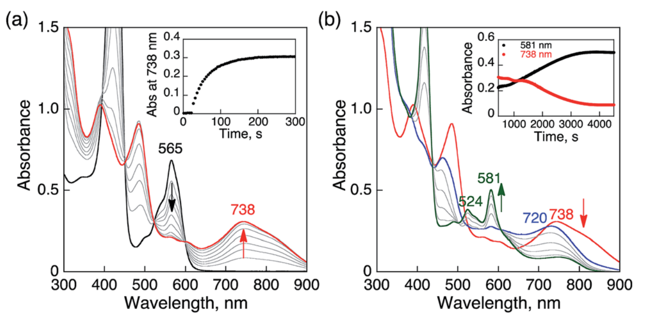


Fig. 6 (a) Absorption spectral changes produced by electron transfer from $Me_8Fc$ ($1.0 \times 10^{-4}$ M) to HTrip ($2.5 \times 10^{-5}$ M) in the presence of $HClO_4$ ($1.0 \times 10^{-4}$ M) in deaerated PhCN at 298 K. (b) Absorption spectral changes upon introducing $O_2$ to a deaerated PhCN solution of (a). The red and green lines show the spectrum of $H_3Trip$ before and after introducing $O_2$ by $O_2$ gas bubbling, respectively. The blue line shows the spectrum due to precursor complex. Insets show absorption time profiles.

HTrip and a large excess of $HClO_4$ resulted in the efficient oxidation of $Me_8Fc$ by $O_2$ to yield $Me_8Fc^+$, as shown in Fig. 7a.

The formation of $Me_8Fc^+$ was monitored by a rise in absorbance at 750 nm due to $Me_8Fc^+$ (Fig. 7b). When an excess amount of $Me_8Fc$ relative to $O_2$ (*i.e.*, [$O_2$] limiting conditions) was employed, the concentration of produced $Me_8Fc^+$ ($1.9 \times 10^{-3}$ M) was twice that of $O_2$ ($9.4 \times 10^{-4}$ M). In addition, the stoichiometric production of $H_2O_2$ was confirmed by iodometric titration, as shown in Fig. S8 (in the ESI†). In contrast, when an excess amount of $O_2$ relative to $Me_8Fc$ (*i.e.*, [$Me_8Fc$] limiting conditions) was employed, the concentration of produced $H_2O_2$ ($1.0 \times 10^{-3}$ M) was half that of $Me_8Fc$ ($2.0 \times 10^{-3}$ M), where the amount of $H_2O_2$ was determined by the reaction with [(TMC)$Fe^{II}$]$(OTf)_2$ (TMC = 1,4,8,11-tetramethyl-

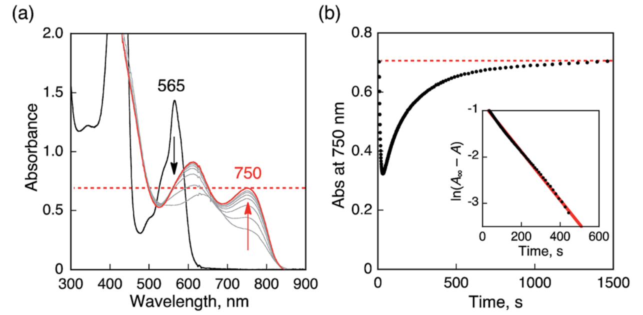


Fig. 7 (a) Absorption spectral changes in the two-electron reduction of $O_2$ ($9.4 \times 10^{-4}$ M) by $Me_8Fc$ ($1.0 \times 10^{-2}$ M) with HTrip ($5.0 \times 10^{-5}$ M) in the presence of $HClO_4$ ($1.0 \times 10^{-2}$ M) in PhCN at 298 K. The black and red lines show the spectra before and after addition of $Me_8Fc$, respectively. The dotted line is the absorbance at 750 nm due to $1.9 \times 10^{-3}$ M of $Me_8Fc^+$. (b) Time profile of absorbance at 750 nm due to $Me_8Fc^+$. Inset shows first-order plot.

1,4,8,11-tetraazacyclotetradecane) to produce the corresponding Fe(IV)-oxo complex ($[(TMC)Fe^{IV}(O)]^{2+}$, as shown in Fig. S9 (in the ESI†).[43] Thus, the stoichiometry of the catalytic reduction of $O_2$ by $Me_8Fc$ has been firmly established, as given in eqn (3).

$$O_2 + 2H^+ + 2Me_8Fc \xrightarrow[\text{HTrip}]{} H_2O_2 + 2Me_8Fc^+ \tag{3}$$

The rate of formation of $Me_8Fc^+$ in the catalytic reduction of $O_2$ with excess $Me_8Fc$ and $HClO_4$ in Fig. 7b obeys first-order kinetics. It should be noted that the oxidation of $Me_8Fc$ by $O_2$ hardly occurred in the absence of HTrip under the present experimental conditions, as shown in Fig. S10 (in the ESI†). When $Me_8Fc$ was replaced by weaker one-electron reductants such as ferrocene (Fc : $E_{ox}$ = 0.37 V *vs.* SCE) and dimethylferrocene ($Me_2Fc$ : $E_{ox}$ = 0.26 V *vs.* SCE), no changes in the absorption band of $H_2Trip^+$ at 565 nm were observed, as shown in Fig. S11 (in the ESI†). When $Me_8Fc$ was replaced by a stronger one-electron reductant, *i.e.*, decamethylferrocene ($Me_{10}Fc$ : $E_{ox}$ = −0.10 V *vs.* SCE), greatly enhanced oxidation of $Me_{10}Fc$ occurred with the decrease in absorbance at 565 nm due to $H_2Trip^+$ (Fig. S12a in the ESI†). In the case of $Me_{10}Fc$, however, the oxidation of $Me_{10}Fc$ by $O_2$ occurred without HTrip in the presence of $HClO_4$ in PhCN (Fig. S12c in the ESI†). These results indicate that the reduction of $H_2Trip^+$ to produce $H_3Trip$ is essential in the catalytic reduction of $O_2$ to produce $H_2O_2$.

When a metal complex of HTrip, $\eta^5$-cyclopentadienyliron(II) [14]triphyrin(2.1.1) ($CpFe^{II}Trip$),[41c] was employed as an $O_2$ reduction catalyst instead of HTrip for comparison, however, the addition of $HClO_4$ to an air-saturated PhCN solution of $CpFe^{II}Trip$ resulted in a spectral change, as shown in Fig. S13 (in the ESI†). The characteristic absorption bands of $CpFe^{II}Trip$ at 545 nm and 608 nm disappeared upon the addition of $HClO_4$ with the appearance of new absorption bands at 565 nm, which can be attributed to those of $H_2Trip^+$. This indicates that $CpFe^{II}Trip$ was easily demetallated and protonated to afford $H_2Trip^+$ in the presence of $HClO_4$, as shown in Fig. S13 (in the ESI†).

### Kinetics and mechanism of the catalytic two-electron reduction of $O_2$ by $Me_8Fc$ with HTrip

The dependence of the first-order rate constant for the formation of $Me_8Fc^+$ on the concentrations of HTrip, $HClO_4$, $Me_8Fc$, and $O_2$ was examined, as shown in Fig. S14 (in the ESI†), where the first-order rate constants were determined from the initial slopes of the first-order plots in order to avoid further complication due to the deactivation of the catalyst during the reactions, as shown in Fig. S15 (in the ESI†). The observed first-order rate constant ($k_{obs}$) was proportional to the concentration of HTrip, whereas the $k_{obs}$ value remained constant irrespective of the concentration of $HClO_4$ or $Me_8Fc$ (Fig. 8). Although no degradation of HTrip occurred under the present acidic conditions (Fig. S16 in the ESI†), the turnover number (TON) based on HTrip was determined to be more than 40 when the lower concentration of HTrip ($1.3 \times 10^{-5}$ M) was employed, as shown in Fig. S14a (in the ESI†). Because the catalytic rate depends only on the concentrations of HTrip and $O_2$, the rate-determining step in the catalytic cycle must be the reaction of $H_3Trip$ with $O_2$ in Scheme 3. The dependence of the initial rate of formation of $Me_8Fc^+$ on the concentration of $O_2$ shows saturation behaviour at large concentrations of $O_2$ (Fig. 8d). Such saturation behaviour is consistent with the formation of the $O_2$ complex ($H_3Trip/O_2$) in the oxidation of $H_3Trip$ with $O_2$ (Fig. 6b and Scheme 3). The overall catalytic cycle is shown in Scheme 3, where proton-coupled electron transfer from $Me_8Fc$ to HTrip is followed by a second electron transfer from $Me_8Fc$ to $H_3Trip^{\bullet+}$ to produce $H_3Trip$, which is slowly oxidized by $O_2$ *via* the $H_3Trip/O_2$ complex as the rate-determining step. Because the direct reaction between $H_3Trip$ and $O_2$ in the $H_3Trip/O_2$ complex is spin-forbidden, the reaction may proceed *via* hydrogen atom transfer from $H_3Trip$ to $O_2$ in the $H_3Trip/O_2$ complex to produce the ($H_2Trip^{\bullet}/HO_2^{\bullet}$) intermediate, followed by a rapid second hydrogen transfer from $H_2Trip^{\bullet}$ to $HO_2^{\bullet}$ to yield $H_2O_2$, accompanied by regeneration of HTrip (Scheme 3). According to Scheme 3, the rate of formation of $Me_8Fc^+$ is given by eqn (4),

$$d[Me_8Fc^+]/dt = k_{cat}[H_3Trip/O_2], \tag{4}$$

where $k_{cat}$ is the rate constant of the hydrogen atom transfer from $H_3Trip$ to $O_2$ in the $H_3Trip/O_2$ complex. Because the concentration of the $H_3Trip/O_2$ complex is given by eqn (5)

$$[H_3Trip/O_2] = K[HTrip][O_2]/(1 + K[O_2]), \tag{5}$$

using the formation constant ($K$), the initial concentration of HTrip, which is converted to $H_3Trip$ in the catalytic reaction, and the concentration of $O_2$, eqn (4) is rewritten as eqn (6).

$$d[Me_8Fc^+]/dt = k_{cat}K[HTrip][O_2]/(1 + K[O_2]) \tag{6}$$

This kinetic equation agrees with the experimental observations in Fig. 8. The $k_{cat}$ and $K$ values were determined from the dependence of the catalytic rate on the concentration of $O_2$ (Fig. 8d) to be 0.5 $s^{-1}$ and $8.4 \times 10^2$ $M^{-1}$, respectively.

Although the radical pair ($H_2Trip^{\bullet}/HO_2^{\bullet}$) in Scheme 3 cannot be detected during the catalytic reaction, the formation of the radical pair ($H_2Trip^{\bullet}/HO_2^{\bullet}$) was successfully detected by EPR measurements using 1-benzyl-1,4-dihydronicotinamide dimer $[(BNA)_2]$[44] as an electron donor to produce $H_3Trip$ under photoirradiation at low temperature. The observed EPR spectrum in aerated PhCN in the presence of $HClO_4$ at low temperature is shown in Fig. 9. A triplet fine structure EPR signal was observed as well as the typical anisotropic signals for $HO_2^{\bullet}$ with the $g_{||}$ value of 2.0341, and isotropic signals for $H_2Trip^{\bullet}$ at 2.0030.[45,46] From the zero-field splitting value ($D$ = 230 G), the distance ($r$) between two unpaired electrons was determined using the relation $D = 27\,800/r^3$ [47] to be 4.9 Å. This distance is consistent with the estimated distance between $O_2$ and $H_3Trip$ in the $H_3Trip/O_2$ complex by DFT calculations (Fig. 9b).

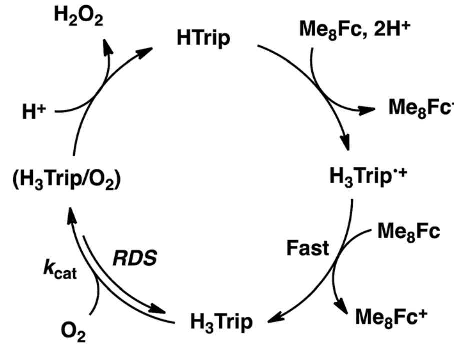


Scheme 3

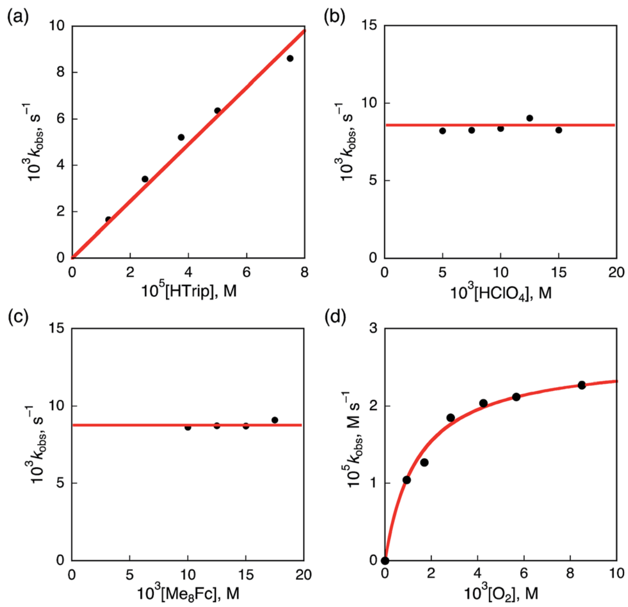


Fig. 8 Plots of (a) $k_{obs}$ *vs.* [HTrip] for the two-electron reduction of $O_2$ ($9.4 \times 10^{-4}$ M) by $Me_2Fc$ ($1.0 \times 10^{-2}$ M) with various concentrations of HTrip in the presence of $HClO_4$ ($1.0 \times 10^{-2}$ M) in PhCN; (b) $k_{obs}$ *vs.* [$HClO_4$] for the two-electron reduction of $O_2$ ($9.4 \times 10^{-4}$ M) by $Me_8Fc$ ($1.0 \times 10^{-2}$ M) with HTrip ($5.0 \times 10^{-5}$ M) in PhCN at 298 K; (c) $k_{obs}$ *vs.* [$Me_8Fc$] for the two-electron reduction of $O_2$ ($9.4 \times 10^{-4}$ M) by various concentrations of $Me_8Fc$ with HTrip ($5.0 \times 10^{-5}$ M) in the presence of $HClO_4$ ($1.0 \times 10^{-2}$ M) in PhCN at 298 K; and (d) $k_{obs}$ *vs.* [$O_2$] for the two-electron reduction of $O_2$ by $Me_8Fc$ ($1.0 \times 10^{-2}$ M) with HTrip ($5.0 \times 10^{-5}$ M) in the presence of $HClO_4$ ($1.0 \times 10^{-2}$ M) in PhCN at 298 K.

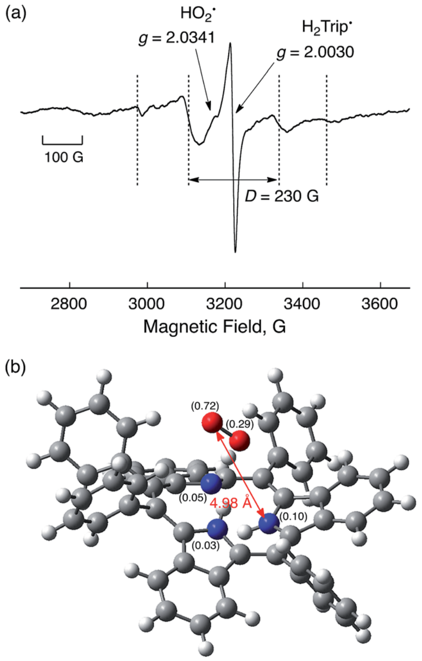


Fig. 9 EPR spectrum observed after the reduction of HTrip ($1.0 \times 10^{-3}$ M) by $(BNA)_2$ ($2.0 \times 10^{-3}$ M) in the presence of $HClO_4$ ($1.0 \times 10^{-3}$ M) in aerated PhCN under photoirradiation using a high-pressure Hg lamp (1000 W) measured at 80 K. Experimental conditions: Microwave frequency 9.0 GHz, microwave power 1.0 mW, modulation frequency 100 kHz, and modulation width 10 G. (b) Optimized structure of $H_3Trip/O_2$ calculated by DFT with calculated spin-density values given in parentheses at the UB3LYP/6-31G(d) level of theory.

# Conclusion

Metal-free triphyrin acts as an efficient catalyst for the two-electron reduction of $O_2$ by $Me_8Fc$ to produce $H_2O_2$ in the presence of $HClO_4$ in PhCN at 298 K. The rate-determining step (RDS) in the catalytic cycle has been found to be hydrogen atom transfer from $H_3Tip$ to $O_2$ in the $H_3Trip/O_2$ complex to produce the radical pair ($H_3Trip^{•+}/HO_2^•$), which was detected as a triplet species by EPR at 80 K. The distance between the two unpaired electrons (4.9 Å) determined from the zero-field splitting constant ($D$) agrees with the distance in the $H_3Trip/O_2$ complex calculated by DFT. The present study provides valuable insight into the catalytic mechanism of the two-electron reduction of $O_2$ with an organic catalyst, and may lead to the development of more efficient metal-free organic catalysts for the selective two-electron reduction of $O_2$ to produce $H_2O_2$.

# Experimental section

## General procedure

Chemicals were purchased from commercial sources and used without further purification, unless otherwise noted. Perchloric acid ($HClO_4$, 70%), trifluoroacetic acid (TFA), ferrocene (Fc), and 1,1-dimethylferrocene ($Me_2Fc$) were purchased from Wako Pure Chemical Industries Ltd. Octamethylferrocene ($Me_8Fc$) and decamethylferrocene ($Me_{10}Fc$) were received from Sigma Aldrich. Fc, $Me_2Fc$, $Me_8Fc$, and $Me_{10}Fc$ were purified by sublimation or recrystallization from ethanol. Benzonitrile (PhCN) used for spectroscopic and electrochemical measurements was distilled over phosphorus pentoxide prior to use.[48] [14]Triphyrin(2.1.1) [HTrip] was synthesized according to the reported procedure.[41] Fe(II)(TMC)(OTf)$_2$ (TMC = 1,4,8,11-tetramethyl-1,4,8,11-tetraazacyclotetradecane; OTf = $CF_3SO_3$) was prepared according to a literature method.[43] Tetra-*n*-butylammonium hexafluorophosphate ($TBAPF_6$) was twice recrystallized from ethanol and dried *in vacuo* prior to use. $^1H$ NMR spectra (300 MHz) were recorded on a JEOL AL-300 spectrometer at room temperature and chemical shifts (ppm) were determined relative to tetramethylsilane (TMS). UV-vis absorption spectroscopy was carried out on a Hewlett Packard 8453 diode array spectrophotometer at room temperature using a quartz cell (light path length = 1 cm).

## Spectroscopic measurements

The amount of hydrogen peroxide ($H_2O_2$) produced was determined by titration with iodide ion: a dilute $CH_3CN$ solution (2.0 mL) of the product mixture (50 μL) was treated with an excess amount of NaI, and the amount of $I_3^-$ formed was determined from the absorption spectrum ($\lambda_{max}$ = 361 nm, $\varepsilon = 2.8 \times 10^4$ $M^{-1}$ $cm^{-1}$).[49] The formation of $H_2O_2$ in the catalytic $O_2$ reduction with HTrip was again confirmed by the reaction between $H_2O_2$ and Fe(II)(TMC)(OTf)$_2$ to afford the corresponding Fe(IV)-oxo species. The amount of the Fe(IV)-oxo species produced was determined from the absorption spectrum ($\lambda_{max}$ = 820 nm, $\varepsilon$ = 400 $M^{-1}$ $cm^{-1}$).[43]

The turnover numbers (TON = the number of moles of $H_2O_2$ formed per mole of HTrip in the catalytic two-electron reduction of $O_2$) were determined from the concentration of produced $Me_8Fc^+$ under catalytic conditions, where stoichiometric production of $H_2O_2$ was confirmed by iodometric titration.

## Kinetic measurements

Rate constants of oxidation of ferrocene derivatives by $O_2$ in the presence of a catalytic amount of HTrip and an excess amount of $HClO_4$ in PhCN at 298 K were determined by monitoring the appearance of an absorption band due to the corresponding ferrocenium ions ($Fc^+$, $\lambda_{max}$ = 620 nm, $\varepsilon_{max}$ = 330 $M^{-1}$ $cm^{-1}$; $Me_2Fc^+$, $\lambda_{max}$ = 650 nm, $\varepsilon_{max}$ = 290 $M^{-1}$ $cm^{-1}$; $Me_8Fc^+$, $\lambda_{max}$ = 750 nm, $\varepsilon_{max}$ = 410 $M^{-1}$ $cm^{-1}$; $Me_{10}Fc^+$, $\lambda_{max}$ = 780 nm, $\varepsilon_{max}$ = 450 $M^{-1}$ $cm^{-1}$).[14] At the wavelengths monitored, spectral overlap was observed with $H_3Trip$ ($\lambda$ = 738 nm ($\varepsilon = 1.6 \times 10^3$ $M^{-1}$ $cm^{-1}$)), $H_3Trip/O_2$ ($\lambda$ = 720 nm ($\varepsilon = 1.2 \times 10^3$ $M^{-1}$ $cm^{-1}$)). The concentration of $O_2$ in an air-saturated PhCN solution was determined to be $1.7 \times 10^{-3}$ M as reported previously.[50] The concentrations of ferrocene derivatives employed for the catalytic reduction of $O_2$ were much larger than that of $O_2$, as $O_2$ is the rate-limiting reagent in the reaction solution. The PhCN solutions containing various concentrations of $O_2$ for the kinetic measurements were prepared by $N_2/O_2$ mixed gas bubbling using a KOFLOC GASBLENDER GB-3C. Typically, a PhCN stock solution of a ferrocene derivative was added using a microsyringe to a PhCN solution containing HTrip and $HClO_4$ in a quartz cuvette (light path length = 1 cm).

### Electrochemical measurements

Cyclic voltammetry (CV) measurements were performed on an ALS 630B electrochemical analyser and voltammograms were measured in deaerated PhCN containing 0.10 M $TBAPF_6$ as a supporting electrolyte at room temperature. A conventional three-electrode cell was used with a glassy carbon working electrode (surface area of 0.3 $mm^2$) and a platinum wire as the counter electrode. The glassy carbon working electrode (BAS) was routinely polished with BAS polishing alumina suspension and rinsed with acetone before use. The potentials were measured with respect to the Ag/$AgNO_3$ ($1.0 \times 10^{-2}$ M) reference electrode. All potentials (*vs.* Ag/$AgNO_3$) were converted to values *vs.* SCE by adding 0.29 V.[51] Redox potentials were determined using the relation $E_{1/2} = (E_{pa} + E_{pc})/2$.

### Spectroelectrochemical measurements

UV-visible spectroelectrochemical experiments were performed with a home-built thin-layer cell (1 mm) that had a light transparent platinum net working electrode. Potentials were applied and monitored with an ALS 730D electrochemical analyser.

### EPR measurements

EPR spectra were measured on a JEOL X-band EPR spectrometer (JES-ME-LX) using a quartz EPR tube containing a deaerated frozen sample solution at 80 K. The internal diameter of the EPR tube is 4.0 mm, which is small enough to fill the EPR cavity but large enough to obtain good signal-to-noise ratios during the EPR measurements at low temperatures (at 80 K). EPR spectrum of $HTrip^{\bullet-}$ produced by the electrochemical reduction of HTrip was measured using a home-built three-electrode quartz EPR tube. Potentials were applied and monitored with an ALS 730D electrochemical analyser. EPR spectra were measured under nonsaturating microwave power conditions. The amplitude of modulation was chosen to optimize the resolution and the signal-to-noise (*S*/*N*) ratio of the observed spectra. The *g* values were calibrated with a $Mn^{2+}$ marker.

### Theoretical calculations

Density functional theory (DFT) calculations were performed on a 32CPU workstation (PQS, Quantum Cube QS8-2400C-064). Geometry optimisations were carried out using the B3LYP/6-31G(d) level of theory[52] for $HTrip^{\bullet-}$, $H_2Trip^+$, $H_3Trip^{2+}$, $H_3Trip^{\bullet+}$, and $[H_3Trip/O_2]$. All calculations were performed using Gaussian 09, revision A.02.[53] Graphical outputs of the computational results were generated with the *GaussView* software program (ver. 3.09) developed by Semichem, Inc.[54]

## Acknowledgements

This work was supported by grants from the Advanced Low Carbon Technology Research and Development (ALCA) and SENTAN programs from Japan Science Technology Agency (JST) to S. F., the Japan Society for the Promotion of Science (JSPS: Grants 26620154 and 26288037 to K. O., 25288092 and 26105004 to H. Y. and 25-727 to K. M.), and the Green Photonics Project in NAIST sponsored by the MEXT (Japan).

## Notes and references

1 (*a*) S. Abrantes, E. Amaral, A. P. Costa, A. A. Shatalov and A. P. Duarte, *Ind. Crops Prod.*, 2007, **25**, 288–293; (*b*) S. H. Zeronian and M. K. Inglesby, *Cellulose*, 1995, **2**, 265–272.

2 L. Li, S. Lee, H. L. Lee and H. J. Youn, *BioResources*, 2011, **6**, 721–736.

3 (*a*) S. Yamazaki, Z. Siroma, H. Senoh, T. Ioroi, N. Fujiwara and K. Yasuda, *J. Power Sources*, 2008, **178**, 20–25; (*b*) R. S. Disselkamp, *Energy Fuels*, 2008, **22**, 2771–2774; (*c*) R. S. Disselkamp, *Int. J. Hydrogen Energy*, 2010, **35**, 1049–1053.

4 S. Fukuzumi, Y. Yamada and K. D. Karlin, *Electrochim. Acta*, 2012, **82**, 493–511.

5 (*a*) Y. Yamada and S. Fukuzumi, *Aust. J. Chem.*, 2014, **67**, 354–364; (*b*) Y. Yamada, M. Yoneda and S. Fukuzumi, *Inorg. Chem.*, 2014, **53**, 1272–1274; (*c*) Y. Yamada, M. Yoneda and S. Fukuzumi, *Chem.–Eur. J.*, 2013, **19**, 11733–11741; (*d*) Y. Yamada, S. Yoshida, T. Honda and S. Fukuzumi, *Energy Environ. Sci.*, 2011, **4**, 2822–2825; (*e*) Y. Yamada, Y. Fukunishi, S. Yamazaki and S. Fukuzumi, *Chem. Commun.*, 2010, **46**, 7334–7336.

6 E. Santacesaria, M. D. Serio, R. Velotti and U. Leone, *Ind. Eng. Chem. Res.*, 1994, **33**, 277–281.

7 M. Fukushima, K. Tatsumi, S. Tanaka and H. Nakamura, *Environ. Sci. Technol.*, 1998, **32**, 3948–3953.

8 S. Liu, K. Mase, C. Bougher, S. D. Hicks, M. M. Abu-Omar and S. Fukuzumi, *Inorg. Chem.*, 2014, **53**, 7780–7788.

9 A. J. Hoffman, E. R. Carraway and M. R. Hoffmann, *Environ. Sci. Technol.*, 1994, **28**, 776–785.

10 (*a*) V. Maurino, C. Minero, G. Mariella and E. Pelizzetti, *Chem. Commun.*, 2005, 2627–2629; (*b*) M. Teranishi, S. Naya and H. Tada, *J. Am. Chem. Soc.*, 2010, **132**, 7850–7851; (*c*) D. Tsukamoto, A. Shiro, Y. Shiraishi, Y. Sugano, S. Ichikawa, S. Tanaka and T. Hirai, *ACS Catal.*, 2012, **2**, 599–603.

11 S. Kato, J. Jung, T. Suenobu and S. Fukuzumi, *Energy Environ. Sci.*, 2013, **6**, 3756–3764.

12 (*a*) Y. Yamada, A. Nomura, K. Ohkubo, T. Suenobu and S. Fukuzumi, *Chem. Commun.*, 2013, **49**, 5132–5134; (*b*) Y. Yamada, A. Nomura, T. Miyahigashi and S. Fukuzumi, *Chem. Commun.*, 2012, **48**, 8329–8331.

13 (*a*) S. Fukuzumi and K. Ohkubo, *Chem. Sci.*, 2013, **4**, 561–574; (*b*) S. Fukuzumi and K. Ohkubo, *Org. Biomol. Chem.*, 2014, **12**, 6059–6071; (*c*) K. Ohkubo and S. Fukuzumi, *Bull. Chem. Soc. Jpn.*, 2009, **82**, 303–315; (*d*) H. Kotani, K. Ohkubo and S. Fukuzumi, *Appl. Catal., B*, 2008, **77**, 317–324; (*e*) K. Ohkubo, R. Iwata, K. Mizushima, K. Souma, Y. Yamamoto, N. Suzuki and S. Fukuzumi, *Chem. Commun.*, 2010, **46**, 601–603.

 

14 (*a*) K. Mase, K. Ohkubo and S. Fukuzumi, *J. Am. Chem. Soc.*, 2013, **135**, 2800–2808; (*b*) T. Honda, T. Kojima and S. Fukuzumi, *J. Am. Chem. Soc.*, 2012, **134**, 4196–4206; (*c*) S. Fukuzumi, *Chem. Lett.*, 2008, **37**, 808–813; (*d*) S. Fukuzumi, K. Okamoto, C. P. Gros and R. Guilard, *J. Am. Chem. Soc.*, 2004, **126**, 10441–10449; (*e*) S. Fukuzumi, K. Okamoto, Y. Tokuda, C. P. Gros and R. Guilard, *J. Am. Chem. Soc.*, 2004, **126**, 17059–17066.

15 (*a*) S. Fukuzumi, S. Mochizuki and T. Tanaka, *Inorg. Chem.*, 1989, **28**, 2459–2465; (*b*) S. Fukuzumi, S. Mochizuki and T. Tanaka, *Inorg. Chem.*, 1990, **29**, 653–659; (*c*) S. Fukuzumi, S. Mochizuki and T. Tanaka, *J. Chem. Soc., Chem. Commun.*, 1989, 391–392.

16 (*a*) R. McGuire Jr, D. K. Dogutan, T. S. Teets, J. Suntivich, Y. Shao-Horn and D. G. Nocera, *Chem. Sci.*, 2010, **1**, 411–414; (*b*) D. K. Dogutan, S. A. Stoian, R. McGuire Jr, M. Schwalbe, T. S. Teets and D. G. Nocera, *J. Am. Chem. Soc.*, 2011, **133**, 131–140; (*c*) T. S. Teets, T. R. Cook, B. D. McCarthy and D. G. Nocera, *J. Am. Chem. Soc.*, 2011, **133**, 8114–8117.

17 (*a*) F. C. Anson, C. Shi and B. Steiger, *Acc. Chem. Res.*, 1997, **30**, 437–449; (*b*) C. Shi, B. Steiger, M. Yuasa and F. C. Anson, *Inorg. Chem.*, 1997, **36**, 4294–4295; (*c*) C. Shi and F. C. Anson, *Inorg. Chem.*, 1998, **37**, 1037–1043; (*d*) Z. Liu and F. C. Anson, *Inorg. Chem.*, 2000, **39**, 274.

18 (*a*) A. Schechter, M. Stanevsky, A. Mahammed and Z. Gross, *Inorg. Chem.*, 2012, **51**, 22–24; (*b*) J. Masa, K. Ozoemena, W. Schuhmann and J. H. Zagal, *J. Porphyrins Phthalocyanines*, 2012, **16**, 761–784.

19 (*a*) A. J. Olaya, D. Schaming, P.-F. Brevet, H. Nagatani, T. Zimmermann, J. Vanicek, H.-J. Xu, C. P. Gros, J.-M. Barbe and H. H. Girault, *J. Am. Chem. Soc.*, 2012, **134**, 498–506; (*b*) P. Peljo, L. Murtomäki, T. Kallio, H.-J. Xu, M. Meyer, C. P. Gros, J.-M. Barbe, H. H. Girault, K. Laasonen and K. Kontturi, *J. Am. Chem. Soc.*, 2012, **134**, 5974–5984; (*c*) B. Su, I. Hatay, A. Trojánek, Z. Samec, T. Khoury, C. P. Gros, J.-M. Barbe, A. Daina, P.-A. Carrupt and H. H. Girault, *J. Am. Chem. Soc.*, 2010, **132**, 2655–2662.

20 (*a*) S. Fukuzumi, S. Mandal, K. Mase, K. Ohkubo, H. Park, J. Benet-Buchholz, W. Nam and A. Llobet, *J. Am. Chem. Soc.*, 2012, **134**, 9906–9909; (*b*) T. Wada, H. Maki, T. Imamoto, H. Yuki and Y. Miyazato, *Chem. Commun.*, 2013, **49**, 4394–4396.

21 (*a*) K. M. Kadish, L. Fremond, J. Shen, P. Chen, K. Ohkubo, S. Fukuzumi, M. El Ojaimi, C. P. Gros, J.-M. Barbe and R. Guilard, *Inorg. Chem.*, 2009, **48**, 2571–2582; (*b*) P. Chen, H. Lau, B. Habermeyer, C. P. Gros, J.-M. Barbe and K. M. Kadish, *J. Porphyrins Phthalocyanines*, 2011, **15**, 467–479; (*c*) K. M. Kadish, L. Fremond, Z. Ou, J. Shao, C. Shi, F. C. Anson, F. Burdet, C. P. Gros, J.-M. Barbe and R. Guilard, *J. Am. Chem. Soc.*, 2005, **127**, 5625–5631.

22 (*a*) C. J. Chang, Y. Deng, D. G. Nocera, C. Shi, F. C. Anson and C. K. Chang, *Chem. Commun.*, 2000, 1355–1356; (*b*) C. J. Chang, Z. H. Loh, C. Shi, F. C. Anson and D. G. Nocera, *J. Am. Chem. Soc.*, 2004, **126**, 10013–10020.

23 (*a*) E. Askarizadeh, S. B. Yaghoob, D. M. Boghaei, A. M. Slawin and J. B. Love, *Chem. Commun.*, 2010, **46**, 710–712; (*b*) M. Volpe, H. Hartnett, J. W. Leeland, K. Wills, M. Ogunshun, B. J. Duncombe, C. Wilson, A. J. Blake, J. McMaster and J. B. Love, *Inorg. Chem.*, 2009, **48**, 5195–5207.

24 (*a*) R. A. Decréau, J. P. Collman and A. Hosseini, *Chem. Soc. Rev.*, 2010, **39**, 1291–1301; (*b*) J. P. Collman, R. Boulatov, C. J. Sunderland and L. Fu, *Chem. Rev.*, 2004, **104**, 561–588.

25 (*a*) J. Rosenthal and D. G. Nocera, *Acc. Chem. Res.*, 2007, **40**, 543–553; (*b*) M. Schwalbe, D. K. Dogutan, S. A. Stoian, T. S. Teets and D. G. Nocera, *Inorg. Chem.*, 2011, **50**, 1368–1377; (*c*) C. J. Chang, L. L. Chng and D. G. Nocera, *J. Am. Chem. Soc.*, 2003, **125**, 1866–1876.

26 (*a*) Z. Halime, H. Kotani, Y. Li, S. Fukuzumi and K. D. Karlin, *Proc. Natl. Acad. Sci. U. S. A.*, 2011, **108**, 13990–13994; (*b*) E. E. Chufan, S. C. Puiu and K. D. Karlin, *Acc. Chem. Res.*, 2007, **40**, 563–572; (*c*) E. Kim, E. E. Chufan, K. Kamaraj and K. D. Karlin, *Chem. Rev.*, 2004, **104**, 1077–1133.

27 (*a*) C. T. Carver, B. D. Matson and J. M. Mayer, *J. Am. Chem. Soc.*, 2012, **134**, 5444–5447; (*b*) B. D. Matson, C. T. Carver, A. von Ruden, J. Y. Yang, S. Raugei and J. M. Mayer, *Chem. Commun.*, 2012, **48**, 11100–11102; (*c*) J. J. Warren, T. A. Tronic and J. M. Mayer, *Chem. Rev.*, 2010, **110**, 6961–7001.

28 (*a*) S. Kakuda, R. L. Peterson, K. Ohkubo, K. D. Karlin and S. Fukuzumi, *J. Am. Chem. Soc.*, 2013, **135**, 6513–6522; (*b*) D. Das, Y.-M. Lee, K. Ohkubo, W. Nam, K. D. Karlin and S. Fukuzumi, *J. Am. Chem. Soc.*, 2013, **135**, 2825–2834; (*c*) D. Das, Y.-M. Lee, K. Ohkubo, W. Nam, K. D. Karlin and S. Fukuzumi, *J. Am. Chem. Soc.*, 2013, **135**, 4018–4026; (*d*) S. Fukuzumi, L. Tahsini, Y.-M. Lee, K. Ohkubo, W. Nam and K. D. Karlin, *J. Am. Chem. Soc.*, 2012, **134**, 7025–7035.

29 (*a*) S. Fukuzumi and K. D. Karlin, *Coord. Chem. Rev.*, 2013, **257**, 187–195; (*b*) L. Tahsini, H. Kotani, Y.-M. Lee, J. Cho, W. Nam, K. D. Karlin and S. Fukuzumi, *Chem.–Eur. J.*, 2012, **18**, 1084–1093; (*c*) S. Fukuzumi, H. Kotani, H. R. Lucas, K. Doi, T. Suenobu, R. L. Peterson and K. D. Karlin, *J. Am. Chem. Soc.*, 2010, **132**, 6874–6875.

30 (*a*) J. Zhang and F. C. Anson, *J. Electroanal. Chem.*, 1993, **348**, 81–97; (*b*) Y. Lei and F. C. Anson, *Inorg. Chem.*, 1994, **33**, 5003–5009; (*c*) Y. C. Weng, F.-R. F. Fan and A. J. Bard, *J. Am. Chem. Soc.*, 2005, **127**, 17576–17577.

31 (*a*) M. S. Thorum, J. Yadav and A. A. Gewirth, *Angew. Chem., Int. Ed.*, 2009, **48**, 165–167; (*b*) C. C. L. McCrory, A. Devadoss, X. Ottenwaelder, R. D. Lowe, T. D. P. Stack and C. E. D. Chidsey, *J. Am. Chem. Soc.*, 2011, **133**, 3696–3699; (*c*) M. A. Thorseth, C. E. Tornow, E. C. M. Tse and A. A. Gewirth, *Coord. Chem. Rev.*, 2013, **257**, 130–139; (*d*) M. A. Thorseth, C. S. Letko, T. B. Rauchfuss and A. A. Gewirth, *Inorg. Chem.*, 2011, **50**, 6158–6161.

32 C. Kemal, T. W. Chan and T. C. Bruice, *J. Am. Chem. Soc.*, 1977, **99**, 7272–7286.

33 (*a*) K. Gong, F. Du, Z. Xia, M. Durstock and L. Dai, *Science*, 2009, **323**, 760–764; (*b*) S. Wang, D. Yu and L. Dai, *J. Am. Chem. Soc.*, 2011, **133**, 5182–5185.

34 (*a*) Q. Li, B. W. Noffke, Y. Wang, B. Menezes, D. G. Peters, K. Raghavachari and L.-S. Li, *J. Am. Chem. Soc.*, 2014, **136**,

3358–3361; (*b*) Y. Jiao, Y. Zheng, M. Jaroniec and S. Z. Qiao, *J. Am. Chem. Soc.*, 2014, **136**, 4394–4403.
35 L. Wang, A. Ambrosi and M. Pumera, *Angew. Chem., Int. Ed.*, 2013, **52**, 13818–13821.
36 (*a*) S. Shibata, T. Suenobu and S. Fukuzumi, *Angew. Chem., Int. Ed.*, 2013, **52**, 12327–12331; (*b*) S. Fukuzumi, K. Yasui, T. Suenobu, K. Ohkubo, M. Fujitsuka and O. Ito, *J. Phys. Chem. A*, 2001, **105**, 10501–10510; (*c*) S. Fukuzumi, S. Kuroda, T. Goto, K. Ishikawa and T. Tanaka, *J. Chem. Soc., Perkin Trans. 2*, 1989, 1047–1053.
37 (*a*) S. Ghisla and V. Massey, *Eur. J. Biochem.*, 1989, **181**, 1–17; (*b*) T. C. Bruice, *Acc. Chem. Res.*, 1980, **13**, 256–262; (*c*) V. Massey, *J. Biol. Chem.*, 1994, **269**, 22459–22462.
38 S. Fukuzumi and T. Okamoto, *J. Chem. Soc., Chem. Commun.*, 1994, 521–522.
39 (*a*) I. Hatay, B. Su, M. A. Méndez, C. Corminboeuf, T. Khoury, C. P. Gros, M. Bourdillon, M. Meyer, J.-M. Barbe, M. Ersoz, S. Záliš, Z. Samec and H. H. Girault, *J. Am. Chem. Soc.*, 2010, **132**, 13733–13741; (*b*) A. Trojánek, J. Langmaier and Z. Samec, *Electrochim. Acta*, 2012, **82**, 457–462; (*c*) A. Trojánek, J. Langmaier, B. Su, H. H. Girault and Z. Samec, *Electrochem. Commun.*, 2009, **11**, 1940–1943; (*d*) S. Wu and B. Su, *Chem.–Eur. J.*, 2012, **18**, 3169–3173; (*e*) X. Liu, S. Wu and B. Su, *J. Electroanal. Chem.*, 2013, **709**, 26.
40 N. Lopez, D. J. Graham, R. McGuire Jr, G. E. Alliger, Y. Shao-Horn, C. C. Cummins and D. G. Nocera, *Science*, 2012, **335**, 450–453.
41 (*a*) Z.-L. Xue, J. Mack, H. Lu, L. Zhang, X.-Z. You, D. Kuzuhara, M. Stillman, H. Yamada, S. Yamauchi, N. Kobayashi and Z. Shen, *Chem.–Eur. J.*, 2011, **17**, 4396–4407; (*b*) Z.-L. Xue, Z. Shen, J. Mack, D. Kuzuhara, H. Yamada, T. Okujima, N. Ono, X.-Z. You and N. Kobayashi, *J. Am. Chem. Soc.*, 2008, **130**, 16478–16479; (*c*) Z.-L. Xue, D. Kuzuhara, S. Ikeda, Y. Sakakibara, K. Ohkubo, N. Aratani, T. Okujima, H. Uno, S. Fukuzumi and H. Yamada, *Angew. Chem., Int. Ed.*, 2013, **52**, 7306–7309.
42 I. Kaljurand, A. Kütt, L. Sooväli, T. Rodima, V. Mäemets, I. Leito and I. A. Koppel, *J. Org. Chem.*, 2005, **70**, 1019–1028.
43 (*a*) J.-U. Rohde, J.-H. In, M. H. Lim, W. W. Brennessel, M. R. Bukowski, A. Stubna, E. Münck, W. Nam and L. Que Jr, *Science*, 2003, **299**, 1037–1039; (*b*) E. S. Yang, M.-S. Chan and A. C. Wahl, *J. Phys. Chem.*, 1975, **79**, 2049–2051.
44 S. Fukuzumi, T. Suenobu, M. Patz, T. Hirasaka, S. Itoh, M. Fujitsuka and O. Ito, *J. Am. Chem. Soc.*, 1998, **120**, 8060–8068.
45 (*a*) K. Suga, K. Ohkubo and S. Fukuzumi, *J. Phys. Chem. A*, 2005, **109**, 10168–10175; (*b*) H. Kotani, K. Ohkubo and S. Fukuzumi, *J. Am. Chem. Soc.*, 2004, **126**, 15999–16006; (*c*) S. Fukuzumi and K. Ohkubo, *Chem.–Eur. J.*, 2000, **6**, 4532–4535.
46 (*a*) R. N. Bagchi, A. M. Bond, F. Scholz and R. Stösser, *J. Am. Chem. Soc.*, 1989, **111**, 8270–8271; (*b*) M. Bersohn and J. R. Thomas, *J. Am. Chem. Soc.*, 1964, **86**, 959–959; (*c*) J. A. Howard, in *Peroxyl radicals*, ed. Z. B. Alfassi, Wiley, Chichester, 1997, p. 283.
47 (*a*) J. S. Park, E. Karnas, K. Ohkubo, P. Chen, K. M. Kadish, S. Fukuzumi, C. W. Bielawski, T. W. Hudnall, V. M. Lynch and J. L. Sessler, *Science*, 2010, **329**, 1324–1326; (*b*) S. Fukuzumi, K. Ohkubo, Y. Kawashima, D. S. Kim, J. S. Park, A. Jana, V. Lynch, D. Kim and J. L. Sessler, *J. Am. Chem. Soc.*, 2011, **133**, 15938–15941.
48 W. L. F. Armarego and C. L. L. Chai, *Purification of Laboratory Chemicals*, Pergamon Press, Oxford, 7th edn, 2013.
49 S. Fukuzumi, S. Kuroda and T. Tanaka, *J. Am. Chem. Soc.*, 1985, **107**, 3020–3027.
50 (*a*) S. Fukuzumi, H. Imahori, H. Yamada, M. E. El-Khouly, M. Fujitsuka, O. Ito and D. M. Guldi, *J. Am. Chem. Soc.*, 2001, **123**, 2571–2575; (*b*) S. Fukuzumi, M. Ishikawa and T. Tanaka, *J. Chem. Soc., Perkin Trans. 2*, 1989, 1037–1045.
51 C. K. Mann and K. K. Barnes, in *Electrochemical Reactions in Non-Aqueous Systems*, Mercel Dekker, New York, 1970.
52 A. D. Becke, *J. Chem. Phys.*, 1993, **98**, 5648–5652.
53 M. J. Frisch, G. W. Trucks, H. B. Schlegel, G. E. Scuseria, M. A. Robb, J. R. Cheeseman, G. Scalmani, V. Barone, B. Mennucci, G. A. Petersson, H. Nakatsuji, M. Caricato, X. Li, H. P. Hratchian, A. F. Izmaylov, J. Bloino, G. Zheng, J. L. Sonnenberg, M. Hada, M. Ehara, K. Toyota, R. Fukuda, J. Hasegawa, M. Ishida, T. Nakajima, Y. Honda, O. Kitao, H. Nakai, T. Vreven, J. A. Montgomery Jr, J. E. Peralta, F. Ogliaro, M. Bearpark, J. J. Heyd, E. Brothers, K. N. Kudin, V. N. Staroverov, R. Kobayashi, J. Normand, K. Raghavachari, A. Rendell, J. C. Burant, S. S. Iyengar, J. Tomasi, M. Cossi, N. Rega, J. M. Millam, M. Klene, J. E. Knox, J. B. Cross, V. Bakken, C. Adamo, J. Jaramillo, R. Gomperts, R. E. Stratmann, O. Yazyev, A. J. Austin, R. Cammi, C. Pomelli, J. W. Ochterski, R. L. Martin, K. Morokuma, V. G. Zakrzewski, G. A. Voth, P. Salvador, J. J. Dannenberg, S. Dapprich, A. D. Daniels, O. Farkas, J. B. Foresman, J. V. Ortiz, J. Cioslowski and D. J. Fox, *Gaussian 09, revision A.02*, Gaussian, Inc., Wallingford, CT, 2009.
54 R. Dennington II, T. Keith, J. Millam, K. Eppinnett, W. L. Hovell and R. Gilliland, *Gaussview*, Semichem, Inc., Shawnee Mission, KS, 2003.

 